national accelerator laboratory

TM-612
0323

Analysis of the Booster Power-Supply Loop

A.G. Ruggiero

Fermilab, September 1975

Summary

An analysis of the Booster power-supply network is presented in this paper with special emphasis on the transmission-line modes.

The largest closed-orbit distortion calculated at the main driving frequency of 15 Hz is of 10 mm peak-to-peak. No large closed-orbit distortions are expected in the proximity of the first resonance of the line at 470 Hz.

The Booster power-supply network[6] is made of 24 cells. One power-supply cell corresponds to one regular magnet cell of four magnets (DFFD) and is made of two units, each of them including a girder with two magnets (one D and one F), one capacitor bank and one choke with two windings. The secondary winding of the choke connects the magnets to the upper bus bars. A typical magnet interconnection in one cell is shown in Fig. 1, where the various elements are shown in terms of their impedance (Z) or of the inverse of their impedance (admittance, Y).

One power-supply cell can be conceived as a 10-terminal network that can be represented by 6x6 transfer matrix M. If we denote by S_1 and S_2 the input and output vectors, we have in the usual matrix notation

$$S_2 = MS_1 .$$

For the six components of S we can take, in the order, the potential difference Δ between the two bus bars, the current difference δ between the two bus bars, the voltage V and the current I feeding the upstream unit of the cell, and the voltage u and the current i feeding the downstream unit of the cell.

All the upstream units are connected with each other in series and so are the downstream units. The direction of the beam motion is from the left to the right of Fig. 1.

The elements of the transfer matrix M can be calculated by solving the current and voltage network equations. For this purpose it is useful to divide one regular cell in smaller sections as shown in Fig. 1, so that one section includes only one basic

element and can be represented by a rather simple 6x6 transfer matrix. A multiplication chain (from the right to the left of Fig. 1) of the matrices of the sections will give the total transfer matrix M.

A magnet has been represented as an impedance in series to an admittance (the index F means F-magnet and the index D means D-magnet). This is correct only in the low frequency range. Ideally $Z = j\omega L$, where $L = 10$ mH is the inductance of the magnet coil, and $Y = 1/j\omega C$, where $C = 50$ nF is the parasitic capacitance to ground[1]. Henceforth, our model is correct for frequencies smaller than $1/2\pi\sqrt{LC} = 7$ kHz, and it does not really matter, in this approximation, where the admittance Y is located compared to the impedance Z (before, after or even in the middle). Similarly, one can also represent the group of the two magnets in the same girder as an impedance in series to an admittance, this being a good approximation for frequencies smaller than $1/2\pi\sqrt{(2L)(2C)} = 3.5$ kHz.

Actually the impedance of a magnet should include also the a.c. resistance due to the coil resistivity and the lamination, as well as the winding capacitance from end-to-end. Extrapolating from some numerical calculations[2,5], we approximate the a.c. resistance with a linear function of the angular frequency ω

$$R_b = (0.03 + 0.00033\ \omega)\ \text{ohm} .$$

The measurement value[1] of the winding capacitance is 10 nF, therefore of negligible contribution to Z for frequencies smaller than 10 kHz. Since we confine our analysis to frequency values up to 1 kHz, we shall regard a magnet impedance as that given by a pure

inductance of 10 mH in series to the ac resistance.

We shall also ignore the voltage divider (Y_v) which is made of a resistor of 10 MΩ of negligible contribution to the magnet admittance Y for frequencies larger than about 1 Hz.

The main failure of this approximation at high frequencies is that a magnet cannot any longer be represented by lumped elements but should be properly described by distributed elements to form a sort of transmission line.

Summarizing, for frequencies in the range 1 Hz - 1 kHz, a regular power-supply cell can be represented by the simplified 10-terminal network of Fig. 2, where

$$Z_1 = Z_2 = j\omega L + R_b = Z_o \quad (L = 20 \text{ mH})$$
$$Y_1 = Y_2 = j\omega L + R_b = Y_o \quad (C = 100 \text{ nF}) \ .$$

This applies to 19 of the 24 cells; in the other five $Z_1 \neq Z_2$ and $Y_1 \neq Y_2$. In the cell which corresponds(*) to the magnetic cell #21 a reference magnet and a resistor of 5 kΩ to ground are added between the two magnets of the downstream girder (see Fig. 3). For this cell we have

$$Z_1 = Z_o$$
$$Y_1 = Y_o$$
$$Z_2 = Z_o + Z_R$$
$$Y_2 = Y_o + Y_R \ .$$

Since the length of the reference magnet is about 1/3 of the length of a regular one, and we scale the impedance and the admittance of this magnet according to its length, we take

(*) A magnetic cell is defined from the middle point of a long-straight section to the middle point of the next long-straight section. The magnetic cell #1 is the first one downstream of the injection point.

$$Z_R = Z_o/6 \qquad \text{and} \qquad Y_R = Y_o/6 + G$$

where $1/G = 5\ k\Omega$. Observe that the contribution of G is predominent at low frequency (15 Hz) but becomes negligible for frequencies larger than 300 Hz.

In the other four cells one has power-supply connections which are actually made, through a filter, between the two magnets of the upstream girder in the magnetic cells #12 and #24 and between the two magnets of the downstream girder in the magnetic cells #1 and #13. In the last cells the polarity of the power supply is reversed compared to the polarity in the first two cells. A typical connection is shown in Fig. 4. We shall look at the effect of the power-supply source later. Now we want to see the effect to the impedances of the addition of the filters. For these four cells one has

$$Y_1 = Y_2 = Y_o$$

and, for the cells #12 and #24

$$Z_1 = Z_o + Z_f$$
$$Z_2 = Z_o$$

and, for the cells #1 and #13

$$Z_1 = Z_o$$
$$Z_2 = Z_o + Z_f.$$

The filter impedance Z_f is

$$Z_f = (j\omega L_f)\ \rho(\omega)$$

where $L_f = 2$ mH and $\rho(\omega)$ is the filter response function[3]. In our

calculations $\rho(\omega)$ has been approximated as a stepwise function which is zero for frequencies larger than 100 Hz and is unit otherwise.

It remains for us to look at the combination choke-capacitor bank. These are shown with more details in Fig. 5 which applies to the upstream unit, the connections to the bus bars being reversed in the downstream unit. J is the current flowing in the secondary winding, a the current in the primary winding and b the current in the capacitor bank of impedance Z_c. Z_{L1} and Z_{L2} are the impedances, respectively, of the primary and secondary windings and Z_M is the mutual inductance impedance. One has the following equations

$$\Delta_2 = \Delta_1$$
$$I_2 = I_1$$
$$V_1 - V_2 = bZ_c$$
$$\delta_2 = \delta_1 - 2J$$

$$a + b = I_1$$
$$bZ_c = aZ_{L1} - JZ_M$$
$$\Delta_1 = JZ_{L2} - aZ_M \ .$$

One can solve the last three equations in terms of a, b and J and insert the result in the third and fourth equations. One obtains

$$V_2 = V_1 - Z_c \frac{I_1(Z_M^2 - Z_{L1}Z_{L2}) + \Delta_1 Z_M}{Z_M^2 - Z_{L1}Z_{L2} - Z_cZ_{L2}}$$

$$\delta_2 = \delta_1 + 2 \frac{I_1 Z_M Z_c + \Delta_1(Z_c + Z_{L1})}{Z_M^2 - Z_{L1}Z_{L2} - Z_cZ_{L2}}$$

Similar equations for the downstream unit are obtained from these by simply replacing Z_M with $-Z_M$.

Measurements done on the choke[1] showed that Z_{L1} and Z_{L2} are essentially an inductance in series to a small resistance and that Z_M^2 equals $Z_{L1}Z_{L2}$ within few per thousand. Then the above equations become, after setting $Z_M = Z_{L1} = Z_{L2}$,

$$V_2 = V_1 \pm \Delta_1$$

$$\delta_2 = \delta_1 \mp 2I_1 - 2\frac{Z_c+Z_M}{Z_M Z_c}\Delta_1$$

where the upper sign applies to the upstream unit and the lower sign to the downstream unit.

The above equations apply in the approximation that the bus bars are perfectly conductive and that the capacitance and inductance between them is neglected. In this approximation V and I as well as u and i do not depend on δ. Also, in the same approximation, Δ is a constant of a value which depends on the boundary conditions.

In conclusion, the transfer matrix M associated to the cell shown in Fig. 2, can be expressed as the product of three matrices

$$M \equiv M_1 M_2 M_3$$

where M_1 and M_2 are the transfer matrices respectively corresponding to the downstream and upstream choke-capacitor bank group, and M_2 is the transfer matrix corresponding to the magnets, namely to the part of the cell shown between the dashed lines in Fig. 2.

From what is said above, we derive

$$M_1 \equiv \begin{pmatrix} 1 & 0 & 0 & 0 & 0 & 0 \\ -2Y_d & 1 & 0 & 0 & 0 & 2 \\ 0 & 0 & 1 & 0 & 0 & 0 \\ 0 & 0 & 0 & 1 & 0 & 0 \\ -1 & 0 & 0 & 0 & 1 & 0 \\ 0 & 0 & 0 & 0 & 0 & 1 \end{pmatrix}$$

$$M_3 \equiv \begin{pmatrix} 1 & 0 & 0 & 0 & 0 & 0 \\ -2Y_u & 1 & 0 & -2 & 0 & 0 \\ 1 & 0 & 1 & 0 & 0 & 0 \\ 0 & 0 & 0 & 1 & 0 & 0 \\ 0 & 0 & 0 & 0 & 1 & 0 \\ 0 & 0 & 0 & 0 & 0 & 1 \end{pmatrix}$$

and

$$M_2 \equiv \begin{pmatrix} 1 & 0 & 0 & 0 & 0 & 0 \\ 0 & 1 & 0 & 0 & 0 & 0 \\ 0 & 0 & 1 & -Z_1 & 0 & 0 \\ 0 & 0 & -Y_1 & 1+Z_1Y_1 & 0 & 0 \\ 0 & 0 & 0 & 0 & 1 & -Z_2 \\ 0 & 0 & 0 & 0 & -Y_2 & 1+Z_2Y_2 \end{pmatrix}$$

Performing the multiplication yeilds

$$M \equiv \begin{pmatrix} 1 & 0 & 0 & 0 & 0 & 0 \\ -2(Y_u+Y_d) & 1 & 0 & -2 & -2Y_2 & 2(1+Z_2Y_2) \\ 1 & 0 & 1 & -Z_1 & 0 & 0 \\ -Y_1 & 0 & -Y_1 & 1+Z_1Y_1 & 0 & 0 \\ -1 & 0 & 0 & 0 & 1 & -Z_2 \\ 0 & 0 & 0 & 0 & -Y_2 & 1+Z_2Y_2 \end{pmatrix}$$

where

$$Y_u = \frac{1-\omega^2 L_c C_u + j\omega R_c C_u}{R_c + j\omega L_c} \quad , \quad Y_u = \frac{1-\omega^2 L_c C_d + j\omega R_c C_d}{R_c + j\omega L_c} \quad .$$

L_c = 40 mH is the inductance of the choke winding, R_c is the a.c. resistance of the choke and C_u and C_d are the capacitance, respectively, of the upstream and downstream capacitor bank. The capacitance is about 8 mF, but the exact value for each bank is obtained by tuning the whole girder so that the magnets inductance is cancelled by the capacitance at the main frequency of 15 Hz to optimize the power transfer at this frequency. For our calculation we approximated the a.c. resistance of the choke with a linear function of ω, namely[6]

$$R_c = (0.025 + 0.00075\ \omega)\ \text{ohm} \ .$$

The first power-supply cell corresponds to cell #7 and the last one to cell #6. At both ends of the chain the two terminals feeding the two units are shorted to each other and the upper bus bars are open. Thus, denoting by the index "in" the initial values and by the index "out" the final values, the boundary conditions are

$$V_{in} = u_{in} \qquad V_{out} = u_{out}$$

$$I_{in} = -i_{in} \qquad I_{out} = -i_{out}$$

and

$$\delta_{in} = \delta_{out} = 0.$$

The power-supply sources can be taken into account by replacing the 6x6 matrix M by a 7x7 matrix (M/f) in the following way[4]

$$(M/F) = \left(\begin{array}{c|c} M & f \\ \hline 0 & 1 \end{array}\right)$$

where M is the ordinary 6x6 transfer matrix and f is the source vector of six components. This vector is usually made of zeros except for those cells which are connected to the power-supply line. In this case they are

$$(0,\ 0,\ V_s,\ -\tfrac{1}{2}Y_1V_s,\ 0,\ 0)$$

when the power supply is connected to the upstream cell unit, and

$$(0,\ Y_2V_s,\ 0,\ 0,\ -V_s,\ \tfrac{1}{2}Y_2V_s)$$

when the power supply is connected to the downstream cell unit, where V_s is the power-supply voltage.

To obtain the transfer-source matrix from one point to another of the ring, one multiplies in order all matrices of the corresponding cells between the two points. One can also calculate the total transfer-source matrix from one end to the other of the 24-cell chain. By applying the proper boundary conditions one can then calculate, for instance, the input voltage-current vector and, in particular, the current feeding the upstream unit of cell #7. The ratio Y_T of this current to the unit of voltage of one of the four power supplies is shown versus frequency in Fig. 6.

At the feeding frequency of 15 Hz, Y_T = 0.97 Ampère/Volt. With a peak voltage of 490 V this corresponds to a peak current of 475 A as it should be.

At higher frequencies, Y_T decreases like with the inverse of the number of Hertz everywhere except in proximity of two resonances

shown in Fig. 6. The first resonance is at 470 Hz and the second one at 930 Hz.

The current excitation at 15 Hz for each individual girder is shown in Fig. 7. One can easily recognize the discontinuity due to the 5 κΩ damping resistor at the location in correspondance to the reference magnet. But the larger discontinuity ($\Delta I/I = 2.4 \times 10^{-4}$) is between the cells #6 and #7 and is due to the fact that these two cells are not immediately, electrically connected.

The closed-orbit distortion due to the current fluctuation from magnet-to-magnet is shown in Fig. 8. The peak-to-peak distortion is of 10.2 mm and, therefore, if not corrected, of some significant effect in the booster performance.

We also calculated the effect of a parasite frequency other than 15 Hz. The peak-to-peak closed-orbit distortion per unit of peak voltage is shown versus frequency in Fig. 9. The values correspond to injection. The distortion decreases linearly with the beam momentum and oscillates at twice the frequency of the driving voltage. Clearly one needs more information about the frequency spectrum of the power-supply sources, but we do not expect any significant effect at high frequency.

The results of further calculations can be summarized in the following.

(i) Removing the 5 κΩ damping resistor makes the 470 Hz resonance sharper as shown by the dashed curve of Fig. 6. Nevertheless, the closed-orbit distortion at high frequency increases only by 41%.

At the fundamental frequency the current discontinuity at the location of the reference magnet disappears by

removing the damping resistor, but the discontinuity between cell #6 and cell #7 still persists ($\Delta I/I = 2.2 \times 10^{-4}$). The pick-to-pick closed-orbit distortion decreases to 8.8 mm and is essentially due to the latter current discontinuity.

(ii) The peak-to-peak closed-orbit distortion at 15 Hz can be minimized by choosing a damping resistor of 20 κΩ. But the improvement is not very large (8.7 mm). At the same time the closed-orbit distortion at higher frequency would increase by only 25%.

When the damping resistor varies from zero to 1 κΩ the peak-to-peak closed-orbit distortion at 15 Hz changes from 24 mm to 20 mm.

(iii) Essentially no changes are found when the reference magnet, the damping resistor and the filters are removed from the analysis.

(iv) If the a.c. resistance of the magnets and chokes is not taken into account, larger closed-orbit distortion occurs at the resonance frequency: 1.2 mm per volt of the driving voltage. The increase at 15 Hz is smaller; the distortion increases up to only 11.3 mm. From this we infer that the 5 κΩ resistor essentially damps the transmission line mode at 15 Hz whereas the high frequency modes are damped by the a.c. resistance of the magnets and chokes.

(v) Because of the filters and the reference magnet, we thought that likely the girders which contain them do not have the capacitor bank properly tuned to compensate also the addition of either the filter or reference magnet inductance. Thus we did calculations for the case these girders were not properly tuned. We found no

appreciable changes.

(vi) In case of shortage of chokes one can also operate the booster with few magnets disconnected from the upper bus. We did calculations for this case and found that if, for instance, both girders of the cell #15 are detached from the upper bus, there is no appreciable change at 15 Hz. At higher frequency the capacitor bank bypasses the choke and adds actually very little contribution to the magnet impedance, so that the behavior of the line is not affected by the connection status to the upper bus.

(vii) Finally, we consider the case where the 19 regular cells, which are not connected to the power supply and do not contain the reference magnet, are all disconnected from the upper bus. Again, as obvious, no effect was found at high frequency. But the closed-orbit distortion is considerably smaller at 15 Hz: 2.3 mm peak-to-peak. This occurs, nevertheless, at the cost of increasing the ring impedance as seen by the power supply ports. The ratio Y_T of the excitation current to one power supply peak voltage is now 0.36, namely three times higher voltage would be required to get the same excitation current. We believe that this can be explained by observing that the a.c. resistance of the choke is put in parallel to the magnet a.c. resistance by the connection to the upper bus. The disconnection, on the other hand, put the two a.c. resistance in series with the effect of increasing the total resistance.

References

1. J. Lackey, private communication, August 1975

2. S. Snowdon, private communication, August 1975

3. A.R. Donaldson, private communication, August 1975

4. L.C. Teng, TM-332, November 1971

5. J.A. Dinkel, TM-201, January 1970

6. "Booster Synchrotron", Booster Staff, TM-405, January 1973

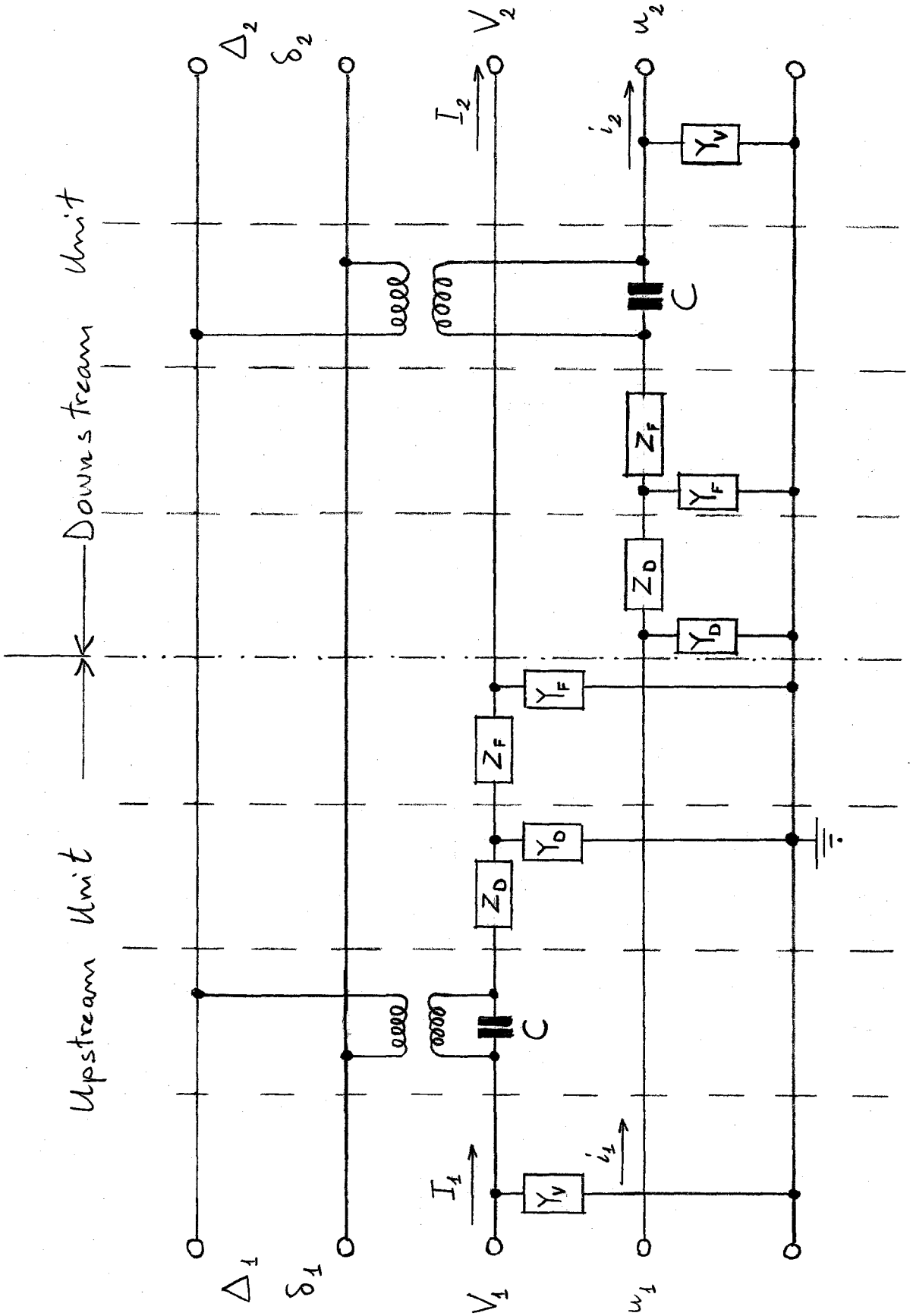
Upstream Unit
Downstream Unit
Δ_1
δ_1
V_1
u_1
Δ_2
δ_2
V_2
u_2
I_1
I_2
i_1
i_2
Y_V
Y_F
Y_D
Z_F
Z_D
C

FIG. 1

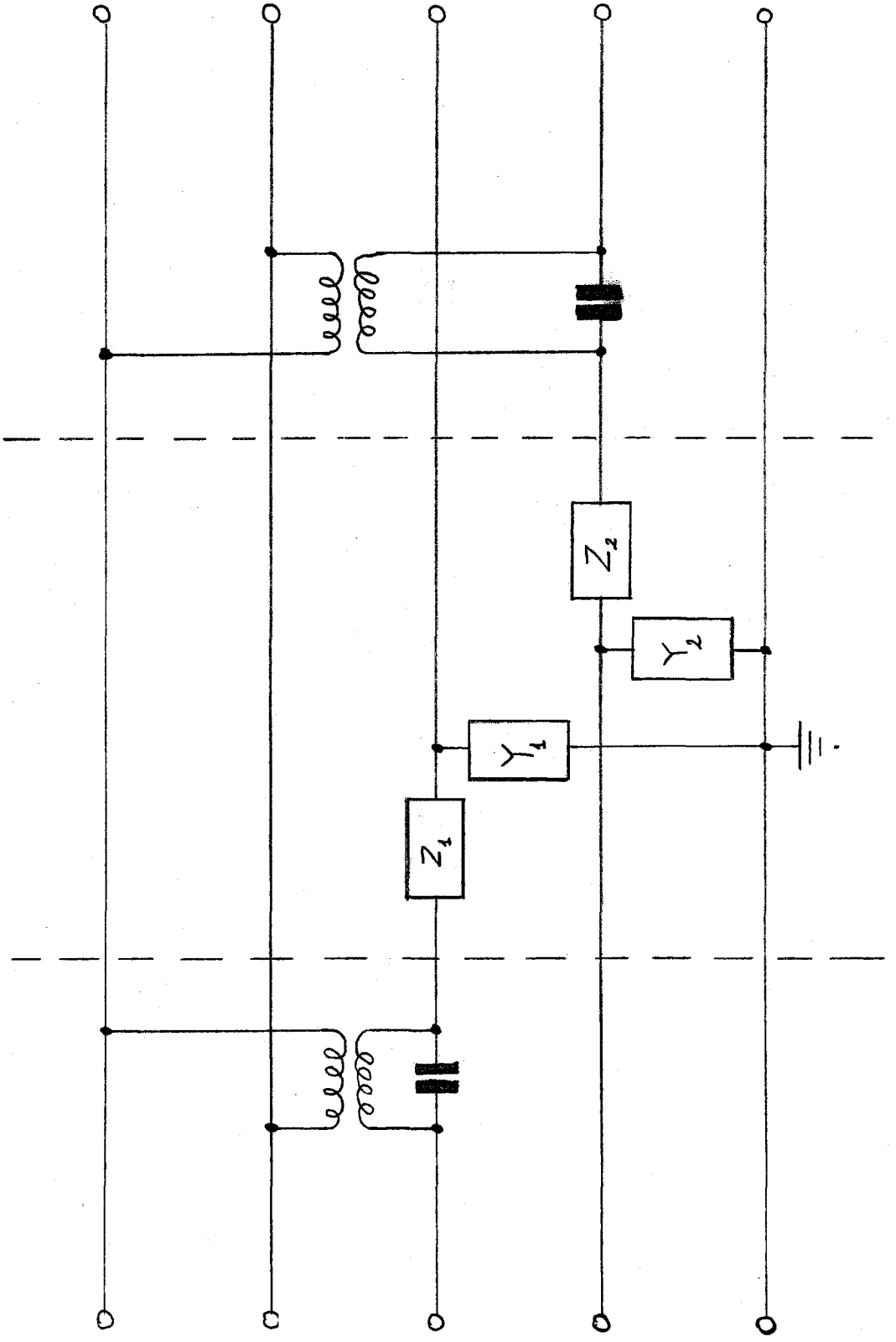

FIG. 2

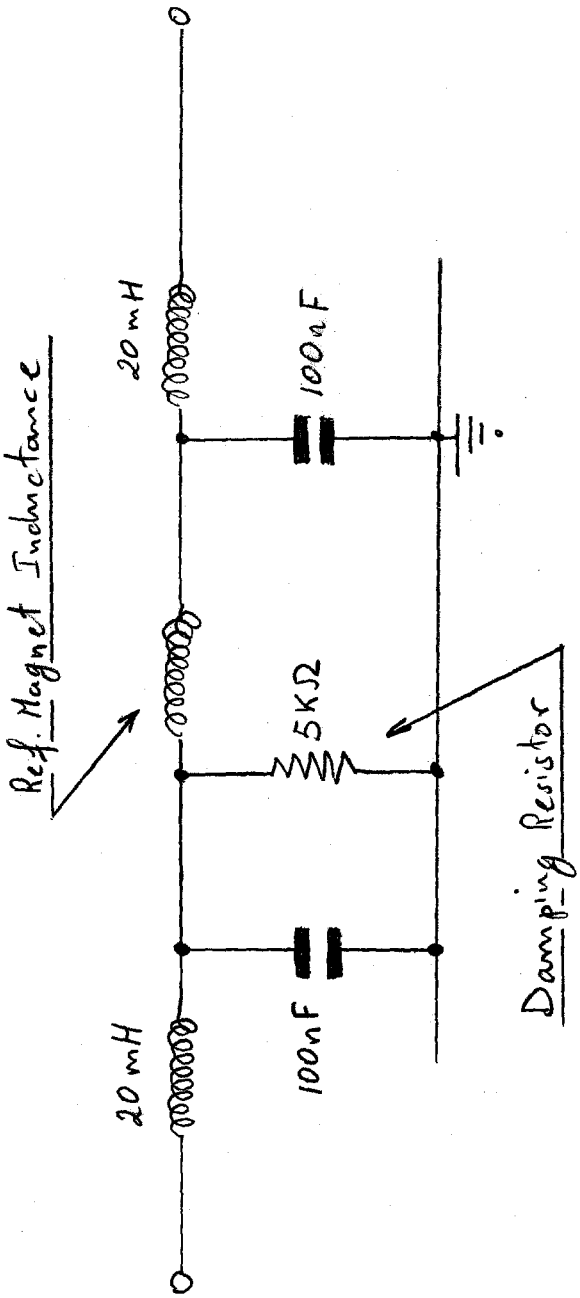
Ref. Magnet Inductance
20 mH
100nF
5KΩ
Damping Resistor
100nF
20 mH

Fig. 3

$L = 0.9\ mH$

$C_1 = 2.4\ mF$

$C_2 = 0.48\ mF$

$R = 1.7\ \Omega$

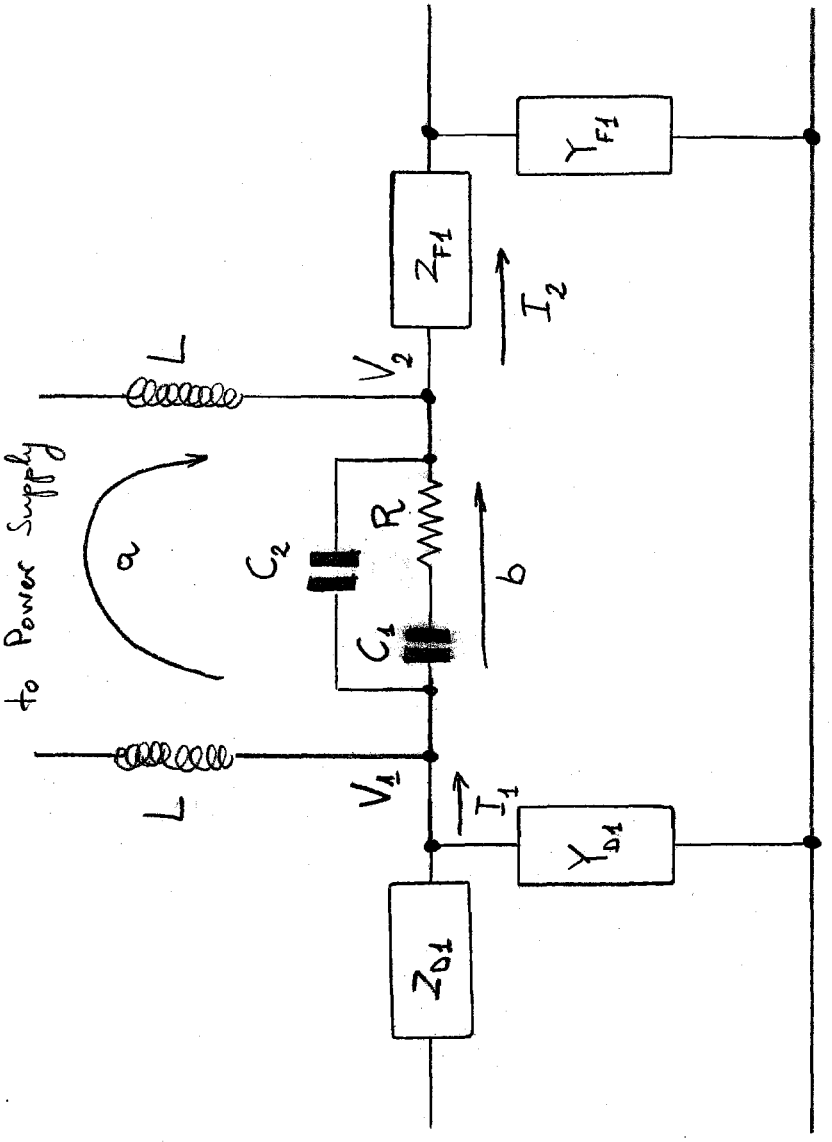

Fig. 4

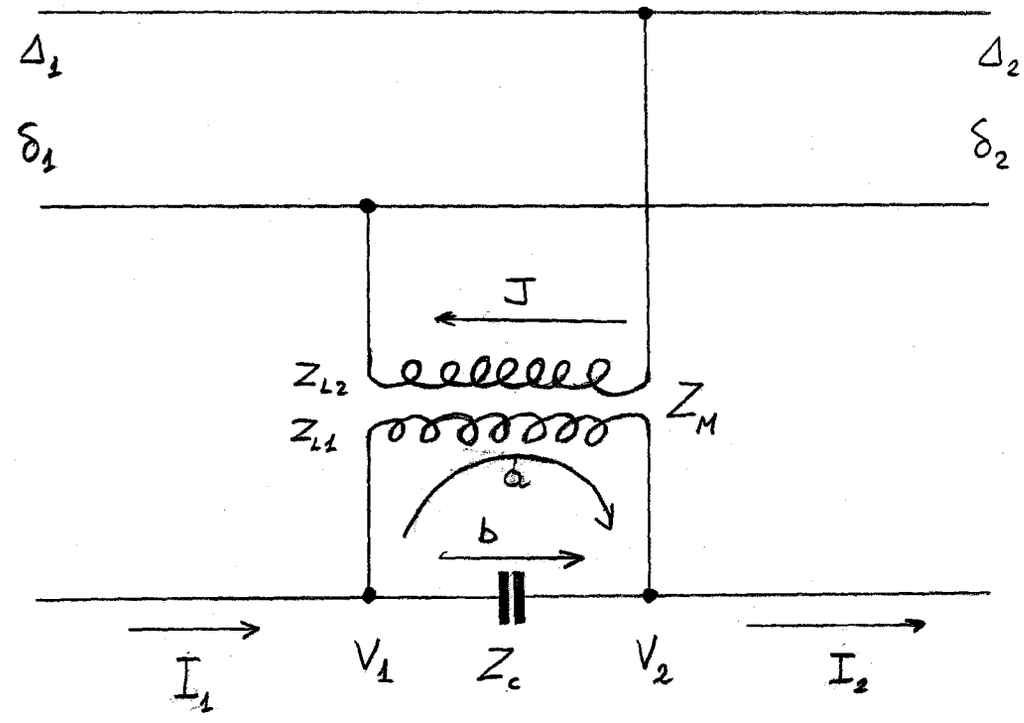

Fig. 5

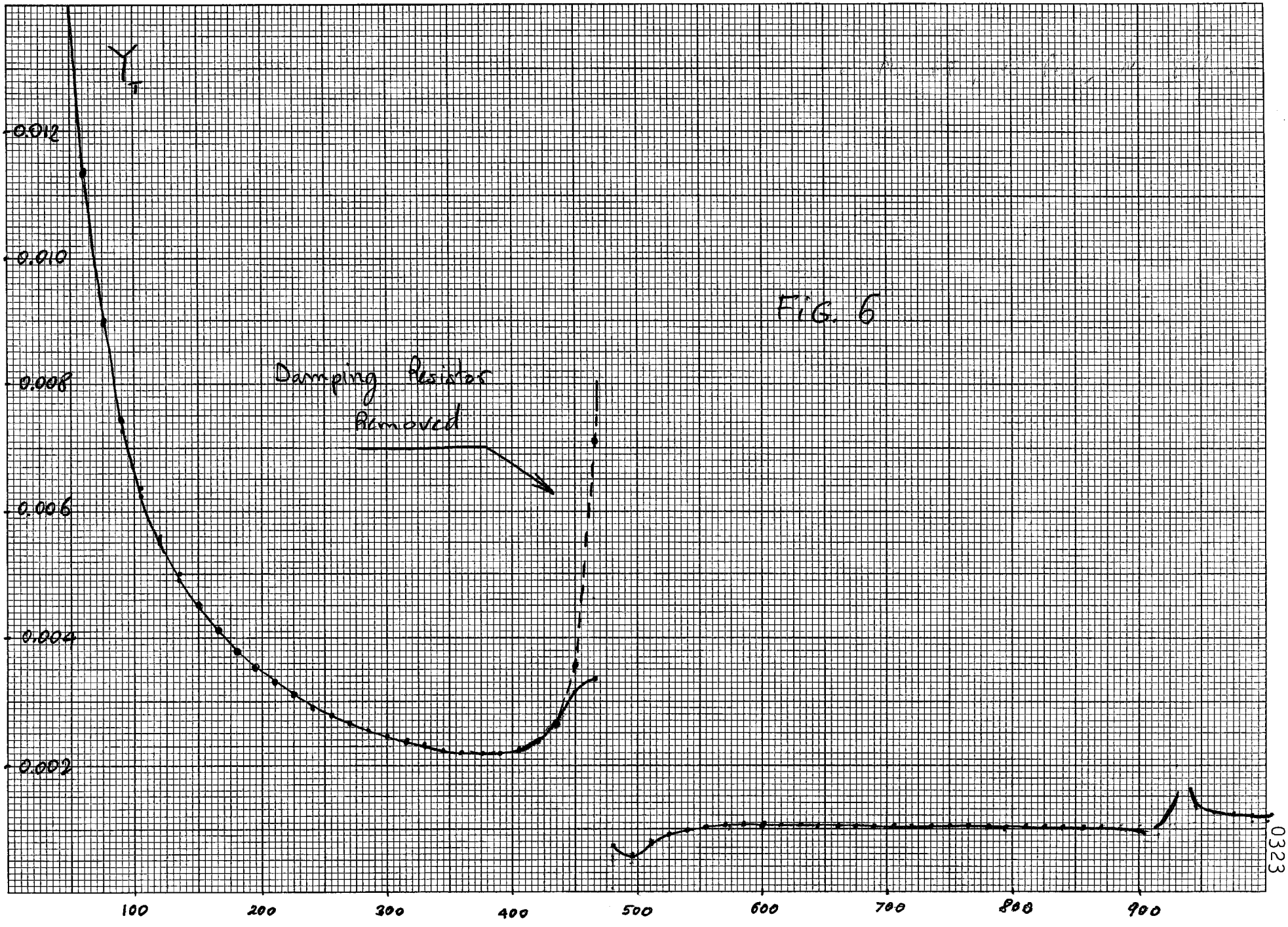

Fig. 6

TM-612
0323

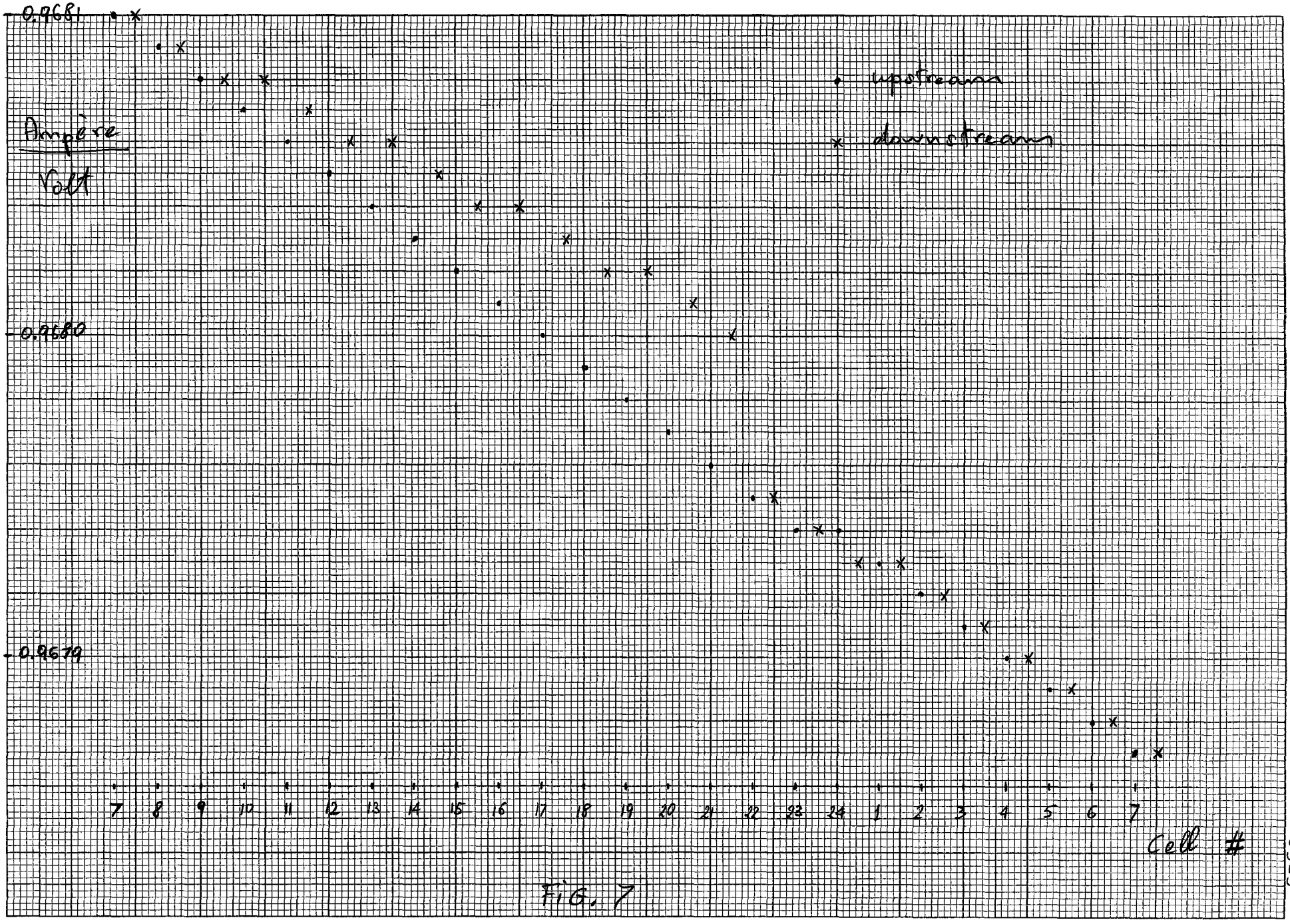
0.9681
0.9680
0.9679
Ampère
Volt
upstream
downstream
7 8 9 10 11 12 13 14 15 16 17 18 19 20 21 22 23 24 1 2 3 4 5 6 7
Cell #

FIG. 7

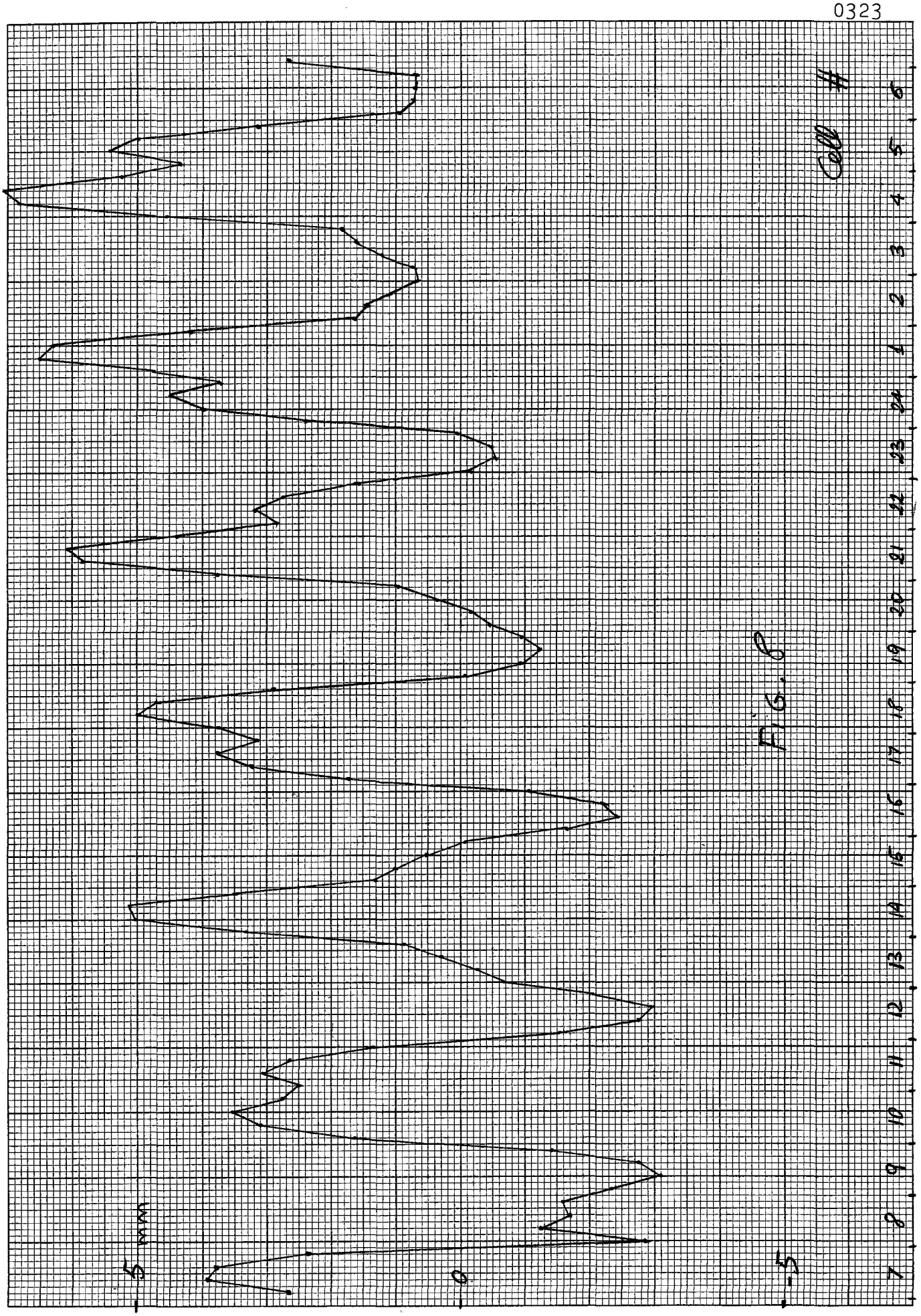

Fig. 6

Peak-to-peak closed circuit voltage
0.2 mm
100
200
300
400
500
600
700
800
900
1000

FIG. 9